PHYSICAL REVIEW B VOLUME 27, NUMBER 4 15 FEBRUARY 1983

Absolute Raman scattering cross sections of *trans*-$(CH)_x$

L. Lauchlan*
Laboratory for Research on the Structure of Matter, University of Pennsylvania, Philadelphia, Pennsylvania 19104 and Department of Materials Science and Engineering, University of Pennsylvania, Philadelphia, Pennsylvania 19104

S. P. Chen and S. Etemad
Laboratory for Research on the Structure of Matter, University of Pennsylvania, Philadelphia, Pennsylvania 19104 and Department of Physics, University of Pennsylvania, Philadelphia, Pennsylvania 19104

M. Kletter
Laboratory for Research on the Structure of Matter, University of Pennsylvania, Philadelphia, Pennsylvania 19104 and Department of Chemistry, University of Pennsylvania, Philadelphia, Pennsylvania 19104

A. J. Heeger
Laboratory for Research on the Structure of Matter, University of Pennsylvania, Philadelphia, Pennsylvania 19104 and Department of Physics, University of Pennsylvania, Philadelphia, Pennsylvania 19104

A. G. MacDiarmid
Laboratory for Research on the Structure of Matter, University of Pennsylvania, Philadelphia, Pennsylvania 19104 and Department of Chemistry, University of Pennsylvania, Philadelphia, Pennsylvania 19104
(Received 23 July 1982; revised manuscript received 12 November 1982)

Measurements of the absolute Raman cross sections for *trans*-$(CH)_x$ are reported. The results have been analyzed to study the contribution of hot luminescence to the inelastically scattered light spectrum. The magnitude and frequency dependence of the absolute scattering cross sections are consistent with hot luminescence being the dominant process. To determine the contribution of static resonance effects (i.e., short chains) to the Raman line shape, we present sliced excitation profiles. We find no evidence for the resonance behavior of short chains.

I. INTRODUCTION

The inelastic scattering spectra (resonance Raman) of *trans*-$(CH)_x$ display characteristic resonance features which have been reported by several groups.[1–3] As the incident frequency is changed from deep-red excitation, the Raman bands broaden and form a shoulder which eventually develops into a prominant second peak for deep-blue excitation. These resonance effects observed in the *trans* isomer have been attributed to the presence of a distribution of chains having varying lengths of π-electron conjugation.[1–4] In that model, the second peak grows in intensity with increasing excitation frequency when chains of shorter conjugation length (and associated π-π^* transition energy) become resonantly enhanced.

Alternatively, in an extension of an earlier calculation performed by Su and Schrieffer,[5] Mele[6] has recently suggested that dynamic effects may contribute to the resonance features in the *trans*-$(CH)_x$ resonance Raman bands described above. Mele proposed that upon photogeneration of an *e-h* pair in the *trans* isomer, the very fast structural relaxation (which eventually leads to the formation of a soliton-antisoliton pair) leaves the system in an excited vibrational state after radiative decay. Energy conservation thus requires that the radiated spectrum contain a Stokes-shifted sideband. Mele predicts that, as the exciting radiation probes further into the valence and conduction bands, the inelastic scattered light spectrum will have the same general features as are observed for *trans*-$(CH)_x$.

Both luminescence and Raman processes may be present and may act competitively as the incident photon frequency approaches the band gap. In general, this raises the question of whether the inelastically scattered light arises from a true Raman process or from luminescence of the real (rather than virtual) excitations; i.e., hot luminescence (HL). The fundamental question is whether there is a physical

difference between these two processes and more importantly whether there is a physical measurement which can be used to distinguish them. Shen[7] distinguishes resonance Raman scattering (RRS) which is a direct, coherent process from hot luminescence which arises from real absorption followed by radiative recombination of the hot carriers. He has shown rigorously that the absolute scattering cross section for a HL process is given by

$$\sigma_{\mathrm{HL}}(\omega)=\sigma_{\mathrm{abs}}(\omega)\frac{\tau_{\mathrm{NR}}(\omega)}{\tau_{\mathrm{R}}} . \quad (1)$$

In this expression, $\sigma_{\mathrm{abs}}(\omega)$ is the absorption cross section, $1/\tau_{\mathrm{NR}}$ is the nonradiative decay rate, and $1/\tau_{\mathrm{R}}$ is the radiative decay rate.

In this paper, we report the results of measurements of the absolute Raman cross sections for *trans*-$(CH)_x$. The results of this measurement have been analyzed to study the contribution of hot luminescence to the inelastically scattered light spectrum. To determine the contribution of static resonance effects (i.e., short chains) to the Raman band line shape, we present the spectral dependence of different frequencies within each band (so-called sliced excitation profiles). We find no evidence for the resonance behavior of short chains. Moreover, the magnitude and frequency dependence of the absolute scattering cross section are consistent with hot luminescence being the dominant process.

II. EXPERIMENTAL

Free standing ($\sim$80 μm thick) *cis*-rich films of polyacetylene were isomerized to the *trans* isomer by heating to 140 °C for about 1 h in vacuum. The samples were then attached to the cold tip of an Air-Products Helitran liquid-flow refrigerator, and the samples were then cooled to approximately 10 K.

The Raman measurements were taken using a Jobin-Yvon Ramanor HG.2S double spectrophotometer equipped with photon-counting detection. Excitation lines from 4762 to 6764 Å were used from a krypton-ion laser. In addition, a coherent radiation dye laser using rhodamine 6G dye was used to obtain excitation lines from 5900 to 6200 Å.

The backscattering geometry (see Fig. 1) used for these experiments was dictated by the high absorption coefficients previously reported for *trans*-polyacetylene and the need for a precisely defined scattering volume. To obtain absolute values of the scattering efficiencies of $(CH)_x$, single crystal α-quartz, of known scattering efficiency, was used as a secondary standard. As shown in Fig. 1, the transparent quartz standard was placed up against the

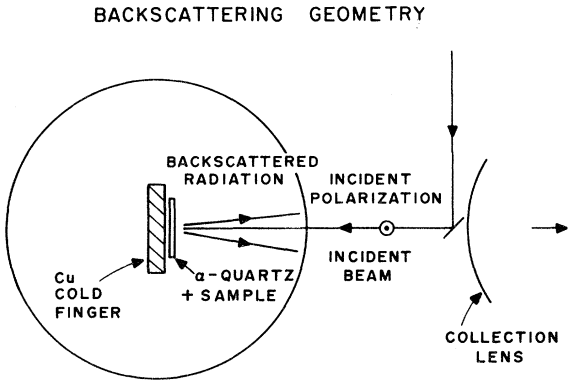

FIG. 1. Backscattering geometry used in the absolute—cross-section measurements.

polyacetylene film during the measurements. The quartz and $(CH)_x$ were then alternately placed at the focus of the collecting lens by means of a micrometer xy translation stage. In this way, the Raman lines of both the α-quartz and polyacetylene were obtained under identical scattering conditions.

As is well known, the intensities which are directly measured in a scattering experiment will be determined by the scattering mechanism as well as by the optical properties, i.e., reflectivity, absorption, and refractive index. For the particular case of resonance scattering, these optical properties are expected to vary with frequency, thereby introducing an extraneous frequency dependence into the measured spectral scattering cross section. It is necessary to account for these material variations when the scattering intensities are compared to those of an external standard with different optical constants. In this way, one may make quantitiative estimates of the absolute magnitudes of the scattering cross sections of vibrational modes which contribute to the inelastic light spectrum. For the present study of resonance scattering from polyacetylene and its comparison with the nonresonance scattering from α-quartz, corrections for the variations of the optical constants of $(CH)_x$ are both necessary and important.

Assuming a planar interface, Callender[8] has shown that, in a backscattering configuration, the corrected intensity I_c is obtained from the measured scattering intensity I_m with the following equation:

$$I_c(\omega_s)=\frac{I_m(\omega_s)[\alpha(\omega_1)+\alpha(\omega_s)]n^2(\omega_s)}{\{[1-R(\omega_1)][1-R(\omega_s)]s(\omega_s)\}} . \quad (2)$$

This expression corrects for the absorption of the laser beam inside the medium, $\alpha(\omega_1)$, and its reflection off the front surface of the material, $R(\omega_1)$; the

absorption of the scattered light, $\alpha(\omega_s)$, and its reflection $R(\omega_s)$; the change in solid angle of light leaving a material with index of refraction n; and the instrumental responsivity $S(\omega_s)$.

The present scattering configuration has required some modification of the above formula in order to take into account the fact that the external standard was present at all times during the course of the measurements. With the use of the scattering configuration shown in Fig. 1, it was necessary to account for the additional reflection losses arising from the polyacetylene-quartz and quartz-vacuum interface.

The index of reflection factor, which appears in Eq. (2) in order to correct for the change in solid angle inside and outside the scatterer, has not been included in the present analysis. The procedure used to polymerize our $(CH)_x$ produces films having one surface which is shiny (formed on the catalyst wetted glass surface) and the opposite surface which is dull (formed in the final stage of polymerization). The integrated raw scattering intensities $[\int I_m(\omega_s)d\omega_s]$ from the shiny and dull surfaces of free-standing films were directly measured and found to be of comparable magnitude (the absolute values are within 20% of each other) throughout the frequency region studied. Since the "dull" surface of a $(CH)_x$ film scatters the incident light diffusely, we conclude that the inelastically scattered light is also diffusely scattered. In the case of diffuse scattering at the surface, the n^2 factor should be omitted from Eq. (2).

The diffuse scattering originates from the shallow penetration depth (a few thousand Å) together with the "rough" underlying fibrillar morphology (fibrils having diameters of approximately 200 Å) of the polymer. Radiation scattered from within a fibril will emerge from the fibril surface in a cone of rays which is normal to the surface. Since the fibrils themselves fill only one third of the film volume and are randomly distributed, the effective cone of radiation is expected to be quite different from that generated from an ideal plane surface. Over the spectral range used in this study, these effects are expected to essentially average out and contribute a constant multiplicative "effective" solid angle correction factor. Since it was not possible to estimate the magnitude of this term, the reported values of the scattering cross sections may be underestimated, although this should not affect the spectral dependence. We note that effects similar to these have been reported by Batchelder *et al.*[9] in their resonance Raman studies of polydiacetylene crystals.

In view of these comments, we have used the following modified formulas to calculate the intrinsic scattering intensities from the experimentally observed intensities. For α-quartz:

$$I_\alpha(\omega_s)=I_m(\omega_s)/([1-R_\alpha(\omega_s)]^2\{1+R_\alpha(\omega_0)+R_{\mathrm{CH}}(\omega_0)[1-R_\alpha(\omega_0)]^2\}S(\omega_s)) . \quad (3)$$

For $(CH)_x$:

$$I_{\mathrm{CH}}(\omega_s)=I_M(\omega_s)[\alpha(\omega_0)+\alpha(\omega_s)]/\{[1-R_{\mathrm{CH}}(\omega_0)][1-R_{\mathrm{CH}}(\omega_s)](1-R_\alpha)^4S(\omega_s)\} . \quad (4)$$

In the above expressions, the corrected intensities for both α-quartz and $(CH)_x$ are obtained by accounting for the reduction in the measured scattering intensity $I_m(\omega_s)$, for the reflection from the quartz surfaces R_α (this has been taken to be 4% throughout the visible), the reflection from the polyacetylene surface, R_{CH}, the absorption of the incident and inelastically scattered light by $(CH)_x$, $\alpha(\omega_0)$, and $\alpha(\omega_s)$, respectively, and the correction for the instrumental responsivity $S(\omega_s)$.

The values for the absorption coefficient and the reflectance have not been obtained directly from the films used in this study. For the absorption coefficient, we have used the low temperature ($T=77$ K) data obtained by Suzuki *et al.*[10] The values for the reflectance from unoriented $(CH)_x$ were obtained from the work of Tanaka *et al.*[11] Values for the absorption coefficient and the reflectance which have been used to correct the measured scattering intensities as a function of frequency in this study are listed in Table I. The instrumental responsivity $S(\omega)$ was directly determined by means of calibrating the spectrometer system with an Optronics model 245C standard quartz-halogen lamp. The absolute scattering cross sections we report are obtained by integrating the area underneath the Raman bands and represent the total contribution of scattering into a particular mode of the polymer. The sliced excitation profiles have been divided by ω^4 in order to separate out the intrinsic resonance function associated with different frequencies within the main line and the prominent shoulder of both the 1070-cm^{-1}

TABLE I. Reflectance and absorption coefficients used to correct the measured scattering intensities for the optical properties of $(CH)_x$ (see text).

λ (Å)	1060 cm^{-1} $R(\lambda)$	1060 cm^{-1} $\alpha(\lambda)\times10^5$	1450 cm^{-1} $R(\lambda)$	1450 cm^{-1} $\alpha(\lambda)\times10^5$
4762	0.19	2.3	0.20	2.3
4825	0.19	2.3	0.20	2.3
5309	0.23	2.6	0.24	2.6
5682	0.25	2.7	0.26	2.8
5905	0.26	2.8	0.27	2.8
6200	0.28	2.7	0.28	2.6
6471	0.28	2.5	0.29	2.3
6764	0.29	2.2	0.30	1.9

and the 1450-cm^{-1} bands.

The scattering efficiency for quartz had been previously measured by Schoen and Cummins.[12] Their value was rechecked by comparing the integrated intensity of the 466-cm^{-1} α-quartz Raman line with that of the 992-cm^{-1} Raman line (of known cross section) of benzene.[13] Our measured value of the cross section for α-quartz agreed to within 20% of the previously reported value.[12] The frequency dependence of the scattering cross section of α-quartz were assumed to follow the expected ω^4 power law in order to compute the scattering efficiency of the standard at different excitation frequencies.

III. EXPERIMENTAL RESULTS AND DISCUSSION

The spectral dependence of the absolute scattering cross section for *trans*-$(CH)_x$ is shown in Fig. 2. The plotted cross section represents the combined scattering efficiencies for the 1070-cm^{-1} mode (an admixture of C-H bend, C=C stretch, and C-C stretch) and the 1450-cm^{-1} mode (principally C=C stretch) over the spectral range from 1.83 to 2.60 eV. The measured cross-section peaks near 2.0 eV with an absolute magnitude approximately equal to 3.0×10^{-24} cm^2/unit cell and falls by a factor of 2 by 2.6 eV. The spectra dependence of the absorption coefficient for *trans*-$(CH)_x$ is shown for comparison in Fig. 2. In this spectral range, the absorption cross section is found to fall by approximately 25% between 2.0 and 2.6 eV.

The Raman cross sections for the individual (1070-cm^{-1}) and (1450-cm^{-1}) bands have been plotted in Fig. 3. From these individual plots, it is seen that the two bands do not exhibit the same frequency dependence. Near 2 eV, the total cross section for the C-C band is almost twice the value measured for the C=C band, whereas at 2.6 eV the measured

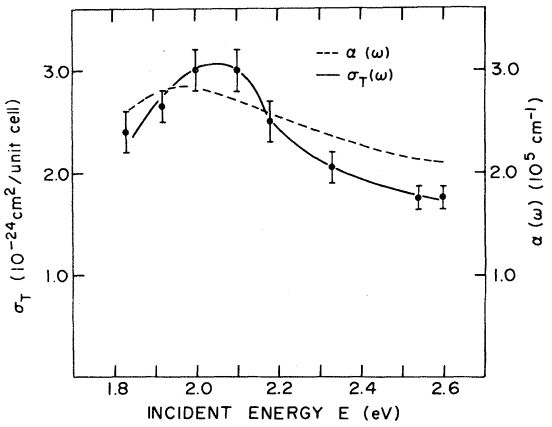

FIG. 2. Absolute cross section for the combined scattering of the C-C (1070-cm^{-1}) and C=C (1450 cm^{-1}) modes as a function of excitation frequency.

values for both cross sections are within 30% of one another. From these plots, it is apparent that the main frequency dependence in the combined scattering cross section is derived from the C-C Raman band (1070 cm^{-1}).

The qualitative similarities between the scattering and absorption cross sections suggest that hot-luminescence processes may dominate the observed inelastic scattering [see Eq. (1)]. Therefore, using Eq. (1), it is useful to estimate τ_{NR} from the measured values for the inelastic scattering (σ_{RR}) and absorption cross sections. For the radiative decay lifetime τ_R we use the value estimated by Mele[14] to be $\sim10^{-7}$ sec. Using $\sigma_{RR}\simeq3\times10^{-24}$ cm^2 and $\sigma_{abs}\simeq10^{-17}$ cm^2, we find $\tau_{NR}\sim10^{-13}$ to 10^{-14} sec.

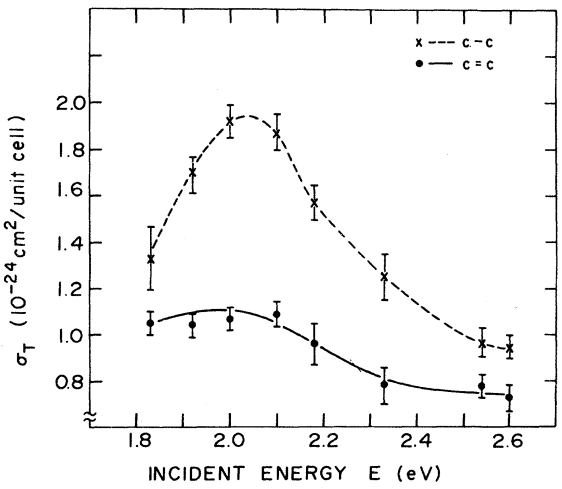

FIG. 3. Absolute cross sections as a function of excitation frequency. The C-C and C=C contributions are plotted separately.

TABLE II. Vibrational frequencies (ν) and π-π^* transition energies (E) for polyenes of various conjugation lengths.

ν (cm^{-1})	$E(n)$ (eV)	n (conjugation lengths)
1460	1.9	50
1470	2.1	22
1490	2.4	11
1510	2.7	8

The value for the nonradiative lifetime is consistent with the time scale predicted for the early stage of evolution of the lattice deformation toward generation of charged solitons from the photogenerated *e-h* pair.[5,6]

The spectral dependence of the scattering cross section does not, however, rule out simple resonance scattering from a static inhomogeneous distribution of chains in the polymer. In order to pursue this question in more detail, we use the sliced excitation profile to investigate the resonance features expected for short chains. In particular, if the variation of the Raman band line shape arises from static effects, the spectral dependence of modes within each band should reflect the associated resonance behavior characteristic of the chain length, as summarized in Table II.[14]

Sliced excitation profiles for both the 1450-cm^{-1} and 1070-cm^{-1} bands of *trans*-$(CH)_x$ are shown in Figs. 4 and 5, respectively. In these plots, increasing

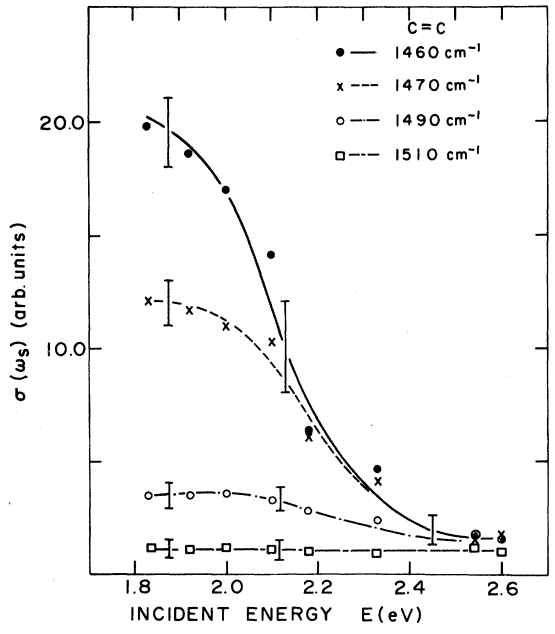

FIG. 4. Sliced excitation profile for the C=C band (1450 cm^{-1}).

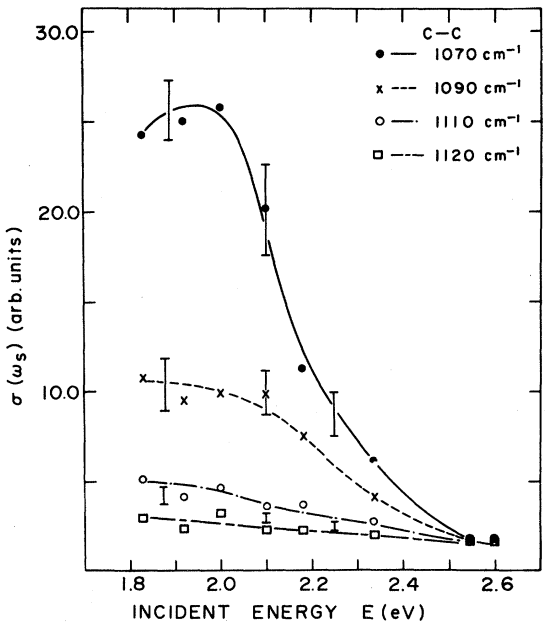

FIG. 5. Sliced excitation profile for the C-C band (1070 cm^{-1}).

vibrational frequency is to be associated with decreasing conjugation length, and therefore with increasing energy gap. As is shown in Table II, the band gaps associated with the selected vibrational frequencies of short-chain polyenes range from 1.9 eV up to 2.7 eV. It is to be expected that as the incident frequency approaches these energies, chains having these conjugation lengths will be selectively enhanced.

These resonance effects are not observed. The scattering near 1460 cm^{-1} shows the strongest frequency variation of the two bands. The scattering cross section falls almost an order of magnitude as the excitation frequency is changed from 1.8 to 2.6 eV. As the selected vibrational frequency is increased, the measured cross sections are reduced in intensity, but do not appear to shift their peak positions. Eventually, for frequencies deep within the second peak of the C=C Raman band, the scattering cross sections become only weakly frequency dependent. This behavior is certainly not expected for a system in which the resonance effects of varying conjugation length dominate the inelastic light scattering.

The sliced excitation profile for the 1070-cm^{-1} band, as shown in Fig. 5, exhibits the same general features observed for the C=C excitation profile. As was observed in the total scattering cross sections, there are differences between the sliced excitation profiles of the two modes. The enhanced

scattering near 2.0 eV is present for all frequencies within this band, although with increasing vibrational frequencies this enhancement becomes progressively weaker. The absence of resonances at higher energies associated with the selected vibrational frequencies in the second peak is consistent with the results obtained from the C=C mode.

The spectral dependence displayed in the excitation profiles of both C-C and C=C bands are different from those previously reported. Fitchen[4] and Lichtman *et al.*[2] presented sliced excitation profiles for the C=C (1450-cm^{-1}) band in *trans*-$(CH)_x$. The profiles presented exhibited enhanced scattering peaks, the positions of which shifted progressively toward higher energies with increasing vibrational frequencies. In their study,[4,15] the sliced excitation profiles of the C=C band were obtained by normalizing the scattered intensity at selected frequencies by the integrated intensity of the *trans* 1290-cm^{-1} line obtained in the same spectrum; i.e., an independent standard was not used. They assumed that the 1290-cm^{-1} line showed no resonance effects in the frequency regime investigated. In view of the absolute—cross-section results presented in this paper, a weak frequency dependence of the 1290-cm^{-1} mode, similar to that observed in the C-C mode, would introduce an apparent frequency dependence in the sliced excitation profile.

The data presented here were obtained from good quality *trans*-$(CH)_x$. Qualitatively similar results were obtained from *trans*-$(CH)_x$ isomerized under less ideal conditions (e.g., 190 °C for 1 h and 240 °C for 1 h). This indicates that moderate variations in the material (as evidenced by changes in the Raman line shape as a result of the more severe isomerization conditions) do not alter the results.

IV. CONCLUSIONS

The weak frequency dependence of the total inelastic light scattering cross section measured for *trans*-$(CH)_x$ is consistent with the interpretation that hot-luminescence processes contribute to the observed inelastic scattering. In the dynamical theory developed by Mele,[6] the fast structural deformation of the lattice in response to the photo-injected *e-h* pair can account for both the line shape (and its variation with varying the excitation frequency) and the resonance behavior observed in the fundamental Raman bands. On the other hand, the sliced excitation profiles do not exhibit a resonance function which shifts as the incident frequency is changed. This feature is inconsistent with selective resonance scattering from a distribution of chains having varying (short) conjugation lengths.

The absence of any resonance features outside of the strong π-π^* transition is also somewhat surprising for the hot-luminescence model. Based on Mele's results,[6] the high-frequency sideband of both modes is predicted to appear with increasing excitation frequency, qualitatively consistent with the experimental data. Unfortunately, there are no predictions currently available regarding the individual resonance profiles associated with the vibrational frequencies within a given mode (for comparison with the sliced excitation profiles). Although resonance effects would be expected, their particular form is not as easily predicted as the correspondence between conjugation length and vibrational frequency. More detailed comparison of the hot-luminescence theory with the experimental results must await definitive calculations of the sliced excitation profiles.

We conclude that the short-chain model, previously used to explain the characteristic Raman line shapes, is ruled out by the absolute—cross-section measurements and the sliced excitation profiles presented in this paper. Our results indicate that hot-luminescence processes may contribute significantly to the enhanced inelastic scattering in *trans*-$(CH)_x$. The resonance Raman line shapes, therefore, may be able to provide detailed information on the early stage of evolution of the lattice deformation toward generation of charged solitons from the photogenerated *e-h* paris.

ACKNOWLEDGMENTS

We thank Professor E. J. Mele for many stimulating and helpful discussions, and Dr. F. Adar and Dr. J. Vanderkooi for use of the Raman spectrometer system on which these experiments were performed. This work was supported by the Army Research Office by Grant No. DAAG 29-81-K-0058.

*Permanent address: IBM Research Laboratory, San Jose, California 95114.

[1]I. Harada, M. Tasumi, H. Shirakawa, and S. Ikeda, Chem. Lett. 1978, 1411 (1978).

[2]L. Lichtmann, D. B. Fitchen, and H. Temkin, Synth. Metals 1, 139 (1979/80).

[3]H. Kuzmany, Phys. Status Solidi G 97, 521 (1980).

[4]D. Fitchen, in Proceedings of the Sixth International Conference on Low Dimensional Conductors, Boulder, Colorado, 1971 [Mol. Cryst. Liq. Cryst. 83, 1127 (1982)].

[5]W. P. Su and J. R. Schrieffer, Proc. Nat. Acad. Sci.

(N.Y.) 77, 5626 (1980).
[6]E. Mele, Solid State Commun. (in press).
[7]Y. R. Shen, Phys. Rev. B 9, 622 (1974).
[8]R. H. Callender, S. S. Sussman, M. Selders, and R. K. Chang, Phys. Rev. B 7, 3788 (1973).
[9]D. N. Batchelder and D. Bloor, J. Phys. C 15, 3005 (1982).
[10]N. Suzuki, M. Ozaki, S. Etemad, A. J. Heeger, and A. G. MacDiarmid, Phys. Rev. Lett. 45, 1209 (1980). For 77 K, only the data near the band edge are shown in the paper. However, data which cover the full range from 0.5 to 4 eV are available.
[11]M. Tanaka, A. Watanabe, and J. Tanaka, Bull. Chem. Soc. Jpn. 53, 3430 (1980).
[12]P. E. Schoen and H. Z. Cummins, in *Light Scattering in Solids,* edited by M. Balkanski (Flammarion, Paris, 1971), p. 560.
[13]J. G. Skinner and W. G. Nilsen, J. Opt. Soc. Am. 58, 113 (1968).
[14]E. Mele (unpublished).
[15]L. S. Lichtmann, Ph.D. thesis, Cornell University, 1981 (unpublished).